ADAPTIVE KALMAN FILTER FOR UAV DYNAMIC FLIGHT MANEUVERS

Kenan Majewski[1] & Marcin Żugaj[1]

[1]Faculty of Power and Aeronautical Engineering, Institute of Aeronautics and Applied Mechanics, Warsaw University of Technology, Warsaw, Poland

Abstract

In this paper, we present an Adaptive Kalman Filter (AKF) designed to enhance the performance of Unmanned Aerial Vehicles (UAVs) in dynamic flight conditions. Traditional Kalman Filters, which assume a constant process noise, often underperform during high-intensity maneuvers due to their static models. The AKF addresses this limitation by dynamically adjusting the process noise covariance based on real-time maneuver detection using data from residuals, acceleration, and gyroscope measurements. We validated the AKF through simulations and real-world tests using the OptiTrack motion capture system, known for its precision in tracking UAV movement. Our results show that the AKF significantly improves state estimation accuracy, reducing root mean square errors (RMSE) compared to conventional Kalman Filters, even during rapid and unpredictable maneuvers. The AKF's adaptability makes it particularly valuable for UAV applications requiring high agility and precision, such as autonomous navigation, obstacle avoidance, and aerial robotics. This paper details the development and evaluation of the AKF, highlighting its potential to set new standards in UAV performance for demanding operational environments.

Keywords: Kalman Filter, UAV Navigation, Maneuver Adaptation, Real-Time Navigation

1. Introduction

1.1 Background and Motivation

Unmanned Aerial Vehicles (UAVs) play a key role in various sectors such as surveillance, delivery, and emergency response operations [1]. Their success depends on accurate navigation and stability, particularly in unpredictable environments. However, conventional navigation systems with static models struggle to adapt to rapid flight condition changes. This has spurred interest in advanced filtering techniques to enhance UAV performance.

1.2 Problem Statement

The Kalman Filter is widely used for state estimation in dynamic systems but falls short during high-intensity maneuvers due to its static model assumptions. To address this, we propose an Adaptive Kalman Filter (AKF) that adjusts the process noise covariance in real time based on detected flight conditions. This improves its responsiveness during aggressive maneuvers, where traditional filters may fail.

1.3 Objective

The objective of this research is to develop an AKF that enhances UAV performance by adapting the process noise covariance in response to detected maneuvers. Unlike traditional methods that assume constant noise levels, the AKF dynamically adjusts the process noise covariance matrix Q using real-time sensor data. This leads to better state estimation accuracy and improved UAV control during rapid maneuvers. The AKF is validated through simulations and real-world testing, setting a new benchmark for UAV performance in demanding environments.

2. Background on Kalman Filters

2.1 Basic Principles of Kalman Filtering

The Kalman Filter is a popular algorithm for estimating the state of a dynamic system from noisy measurements. It works by predicting the system's future state using a model, then correcting that prediction with new measurements [2]. This process repeats over time, with each new measurement improving the accuracy of the estimate. The main strength of the Kalman Filter is its ability to balance predictions and measurements based on their uncertainties, which minimizes the overall error. This makes it efficient for real-time use, as it updates the estimate without needing to store past data. However, the Kalman Filter assumes that both the process noise and measurement noise follow Gaussian distributions with known properties. When this assumption is violated, its performance may suffer.

In real-world applications, like UAV navigation, system dynamics are often nonlinear, making the standard Kalman Filter unsuitable. The Extended Kalman Filter (EKF) is a modified version that handles nonlinearity by linearizing the system around the current estimate [3]. Although this introduces some approximation errors, the EKF is still highly effective for nonlinear systems while keeping the same recursive structure as the standard Kalman Filter.

2.2 Mathematical Formulation

The Kalman Filter algorithm is typically formulated as a two-step process: prediction and update. In the prediction step, the current state and uncertainty are propagated forward using the system's dynamic model. Mathematically, this is expressed as:

$$\begin{aligned} \hat{\boldsymbol{x}}_{k|k-1} &= \boldsymbol{A}\boldsymbol{x}_{k-1|k-1} + \boldsymbol{B}\boldsymbol{u}_{k-1} \\ \boldsymbol{P}_{k|k-1} &= \boldsymbol{A}\boldsymbol{P}_{k-1|k-1}\boldsymbol{A}^T + \boldsymbol{Q}_{k-1} \end{aligned} \tag{1}$$

where the subscript $k|k-1$ indicates predictions or estimates at the current time step k, based on information from the previous time step $k-1$. The predicted state estimate, $\hat{\boldsymbol{x}}k|k-1$, represents the system's expected state before incorporating the latest measurement, while $\boldsymbol{P}k|k-1$ denotes the predicted covariance, reflecting the uncertainty in that prediction, $\boldsymbol{A}$ is the state transition matrix, $\boldsymbol{B}$ is the control input matrix, $\boldsymbol{u}_{k-1}$ is the control input, and $\boldsymbol{Q}_{k-1}$ represents the process noise covariance matrix.

The update step incorporates new measurements to refine the predicted state estimate. First, the innovation $\boldsymbol{s}_k = \boldsymbol{z}_k - \boldsymbol{H}\hat{\boldsymbol{x}}_{k|k-1}$ is calculated, where $\boldsymbol{z}_k$ is the new measurement and $\boldsymbol{H}$ is the observation matrix. The innovation covariance $\boldsymbol{S}_k$ is then computed as:

$$\boldsymbol{S}_k = \boldsymbol{H}\boldsymbol{P}_{k|k-1}\boldsymbol{H}^T + \boldsymbol{R}_k \tag{2}$$

where $\boldsymbol{R}_k$ represents the measurement noise covariance. The Kalman gain $\boldsymbol{K}_k$, which determines how much weight should be given to the new measurement versus the prediction, is calculated as:

$$\boldsymbol{K}_k = \boldsymbol{P}_{k|k-1}\boldsymbol{H}^T\boldsymbol{S}_k^{-1} \tag{3}$$

Finally, the updated state and covariance estimates are given by:

$$\begin{aligned} \hat{\boldsymbol{x}}_{k|k} &= \hat{\boldsymbol{x}}_{k|k-1} + \boldsymbol{K}_k\left[\boldsymbol{z}_k - \boldsymbol{H}\hat{\boldsymbol{x}}_{k|k-1}\right] \\ \boldsymbol{P}_{k|k} &= \boldsymbol{P}_{k|k-1} - \boldsymbol{K}_k\boldsymbol{S}_k\boldsymbol{K}_k^T \end{aligned} \tag{4}$$

This recursive process enables the filter to continuously update its estimate of the system's state, effectively balancing the uncertainties from predictions and measurements to achieve optimal state estimation.

The standard Kalman Filter assumes linearity in the system, meaning that both state transitions and observations can be represented as linear functions. However, many real-world systems, such as UAVs, exhibit nonlinear dynamics. In these cases, the EKF is applied, which extends the Kalman Filter to nonlinear systems by linearizing the state transition and measurement functions at each iteration using a first-order Taylor expansion.

In the EKF, the system model is described by nonlinear functions:

$$\begin{aligned} \hat{\boldsymbol{x}}_{k|k-1} &= f(\hat{\boldsymbol{x}}_{k-1|k-1}, \boldsymbol{u}_{k-1}, \boldsymbol{w}_{k_1}) \\ \boldsymbol{z}_k &= h(\hat{\boldsymbol{x}}_k, \boldsymbol{v}_k) \end{aligned} \tag{5}$$

where $f(\cdot)$ and $h(\cdot)$ are nonlinear functions representing the system's dynamics and measurement model, respectively. To incorporate these nonlinearities into the Kalman Filter framework, the EKF approximates the system around the current estimate by linearizing $f(\cdot)$ and $h(\cdot)$ using the Jacobian matrices. These matrices, $\boldsymbol{F}_k$ and $\boldsymbol{H}_k$, are the partial derivatives of f and h with respect to the state variables, evaluated at the current estimate:

$$\boldsymbol{F}_{k-1} = \frac{\partial f}{\partial \boldsymbol{x}}\Big|_{\hat{\boldsymbol{x}}_{k-1|k-1}}, \quad \boldsymbol{H}_k = \frac{\partial h}{\partial \boldsymbol{x}}\Big|_{\hat{\boldsymbol{x}}_{k|k-1}} \tag{6}$$

The EKF follows the same prediction-update cycle as the standard Kalman Filter, with the linearization applied uring each iteration to handle nonlinear dynamics. This allows the EKF to maintain the recursive, optimal estimation structure while accounting for nonlinearities.

2.3 Applications in UAVs

Kalman Filters play a central role in the navigation and control systems of Unmanned Aerial Vehicles (UAVs), where they are crucial for sensor fusion and real-time state estimation. UAVs often rely on multiple onboard sensors, such as accelerometers, gyroscopes, GPS, barometers, and magnetometers, to estimate key state variables like position, velocity, and orientation. The Kalman Filter optimally integrates the data from these sensors, ensuring accurate state estimation even in the presence of noisy or incomplete measurements.

A key application of Kalman Filters in UAVs is position estimation. In environments where GPS signals are unreliable—such as indoor spaces [4] or urban canyons—the Kalman Filter fuses data from GPS and inertial sensors (e.g., accelerometers and gyroscopes) to maintain an accurate position estimate. This is essential for reliable navigation when GPS data becomes intermittent or degraded. By continuously updating the position estimate with new sensor data, the Kalman Filter allows the UAV to navigate smoothly, even in challenging environments .

Another critical application is attitude determination [5], where the Kalman Filter helps calculate the UAV's orientation (roll, pitch, and yaw). By fusing gyroscope data (which measures angular velocity) with accelerometer and magnetometer readings, the filter corrects for sensor drift and noise, ensuring accurate and stable flight control. Without such filtering, sensor drift would accumulate over time, leading to significant errors in orientation and flight performance.

Kalman Filters are also integral to autonomous UAV navigation. In missions requiring decision-making without human intervention—such as search-and-rescue or delivery operations—the Kalman Filter provides continuous state updates, allowing the UAV to adjust its flight path based on real-time feedback. This capability is crucial for navigating dynamic environments, avoiding obstacles, and adapting to changing conditions such as wind or weather.

3. Methodology

3.1 Adaptive Kalman Filter (AKF)

The Adaptive Kalman Filter (AKF) extends the traditional Kalman Filter by introducing a mechanism to dynamically adjust the process noise covariance matrix, Q_k, during flight maneuvers. In standard Kalman Filters, Q_k is typically fixed, which can lead to suboptimal performance, especially during rapid or aggressive maneuvers when system uncertainty increases. The AKF addresses this by detecting these maneuvers and adjusting Q_k in real time, ensuring robust state estimation accuracy even under dynamic flight conditions.

3.2 Maneuver Detection Algorithm

The AKF relies on a maneuver detection algorithm to identify moments when the UAV experiences significant changes in motion, such as rapid accelerations or rotations. This detection process is essential for triggering adjustments to the filter's process noise. The algorithm continuously monitors

real-time data from the UAV's onboard accelerometers, gyroscopes, and the Kalman Filter's residuals. When these inputs exceed predefined thresholds, the algorithm classifies the event as a maneuver. Maneuvers are detected by analyzing the normalized square of the residual, computed as [6]:

$$\varepsilon = \boldsymbol{s}_k^T \boldsymbol{S}_k^{-1} \boldsymbol{s}_k \tag{7}$$

where the residual $\boldsymbol{s}_k$ represents the difference between the predicted and actual measurements:

$$\boldsymbol{s}_k = \boldsymbol{z}_k - \boldsymbol{H}_k \hat{\boldsymbol{x}}_{k|k-1} \tag{8}$$

and $\boldsymbol{S}_k$ is the system uncertainty, calculated as:

$$\boldsymbol{S}_k = \boldsymbol{H}_k \boldsymbol{P}_{k|k-1} \boldsymbol{H}_k^T + \boldsymbol{R}_k \tag{9}$$

This normalized residual ε serves as a measure of how well the Kalman Filter is performing. Large values of ε indicate a deviation between predicted and observed measurements, signaling potential maneuvers.

Once the residual exceeds a certain predefined threshold, the algorithm interprets this as a maneuver. When this happens, the process noise covariance matrix Q_k is modified in real time to reflect the increased uncertainty in system dynamics. This ensures the AKF can maintain accurate state estimation even during periods of rapid motion or aggressive flight.

In addition to residual monitoring, the algorithm evaluates acceleration and gyroscope data. Maneuvers are flagged if the combined magnitude of acceleration or angular velocity surpasses defined thresholds:

$$\begin{aligned} a_x^2 + a_y^2 + a_z^2 &> a_{threshold} \\ g_x^2 + g_y^2 + g_z^2 &> g_{threshold} \end{aligned} \tag{10}$$

where a_x, a_y, a_z are the acceleration components, and g_x, g_y, g_z are the angular velocities measured by the gyroscope. If either condition is met, the algorithm detects a rapid change in motion, indicating a maneuver.

3.3 Adaptive Process Model

Once a maneuver is detected, the AKF dynamically adjusts the process noise covariance matrix Q_k to better reflect the increased uncertainty in the system dynamics. The process noise is adapted in real-time, ensuring that the filter remains accurate during both normal and aggressive flight.

The adaptive update to Q_k is governed by the following equation:

$$\boldsymbol{Q}_k = \rho(\boldsymbol{Q}_{maneuver}) + (1-\rho)\boldsymbol{Q}_{nominal} \tag{11}$$

In stable flight, ρ starts at 0, meaning the filter relies entirely on $\boldsymbol{Q}_{nominal}$ When a maneuver is detected, ρ increases by 0.1 in each cycle, up to a maximum of 1. This allows the filter to smoothly transition towards using $\boldsymbol{Q}_{maneuver}$, reflecting the higher uncertainty during aggressive motions.

Conversely, when no maneuvers are detected, ρ decreases by 0.01 per cycle until it returns to 0, effectively transitioning back to using $\boldsymbol{Q}_{nominal}$ as the system stabilizes. This gradual change in ρ ensures that the filter adapts smoothly, without sudden jumps in performance, maintaining robust state estimation throughout different flight conditions.

The real-time adaptation of Q_k based on ρ allows the AKF to remain responsive and accurate across a wide range of flight conditions. During aggressive maneuvers, when the system's dynamics are highly uncertain, the filter dynamically increases its process noise to account for the increased variability in state transitions. Conversely, during steady flight, the process noise is reduced, ensuring the filter remains precise and minimizes estimation errors. This adaptability makes the AKF particularly suited for UAV operations requiring high agility and precision, such as obstacle avoidance, autonomous navigation, and complex maneuvers in challenging environments.

4. Experimental UAV Setup

In this section, we describe the experimental setup used to validate the Adaptive Kalman Filter (AKF) for UAV flight. The platform, environment, and quadrotor model are discussed in detail, followed by a summary of the key equations governing the system dynamics.

4.1 Vehicle Platform

The experimental UAV platform used in this study is the Quanser QDrone, a high-performance, mid-size quadrotor designed specifically for indoor laboratory environments (see Figure 1). The QDrone is part of the Autonomous Vehicles Research Studio and is equipped with a powerful onboard Intel® Aero Compute Board, multiple high-resolution cameras, and built-in Wi-Fi. The drone is ideal for advanced research applications, including multi-agent systems, swarm robotics, and vision-based navigation tasks.

Figure 1 – QDrone: High-performance indoor quadrotor.

The QDrone's lightweight yet durable carbon-fiber frame ensures high maneuverability, and its design allows it to withstand high-impact applications with minimal downtime required for repairs. Additionally, the vehicle's onboard processor, RGB-D, and optical flow cameras enable high-quality onboard video processing, with the ability to stream video for real-time monitoring. This makes the QDrone well-suited for precise control and feedback in the controlled indoor environments used for the experiments.

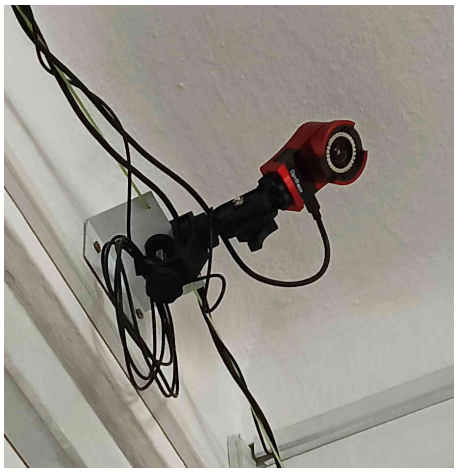

Figure 2 – Optitrack: Infrared motion capture camera.

In addition to its visual sensors, the QDrone is equipped with an onboard Inertial Measurement Unit (IMU), which includes three-axis accelerometers and gyroscopes. These sensors were crucial for this research, providing real-time measurements of linear acceleration and angular velocity in the vehicle's body frame. The data from the IMU was used for state estimation, aiding in the implementation of the

Adaptive Kalman Filter (AKF) by providing essential inputs for the filter to estimate position, velocity, and orientation during flight.
As with other quadrotors, vehicle control is achieved by adjusting the speed of the four rotors through pulse-width modulation (PWM), which governs thrust and torque. The onboard systems communicate with a ground-station PC via Wi-Fi, facilitating high-speed data transfer and enabling precise control during flight testing.

4.2 Optitrack Operating Environment

The flight experiments were conducted indoors, within a controlled environment in a flight testing laboratory. Due to the indoor setting, GNSS (Global Navigation Satellite System) signals were unavailable. Instead, the Optitrack motion capture system (shown in Figure 2) was employed [7] to provide high-accuracy position and attitude feedback. The system uses multiple infrared cameras placed a round the flight volume to track reflective markers on the vehicle, ensuring that at least three cameras have line of sight to the markers at all times.

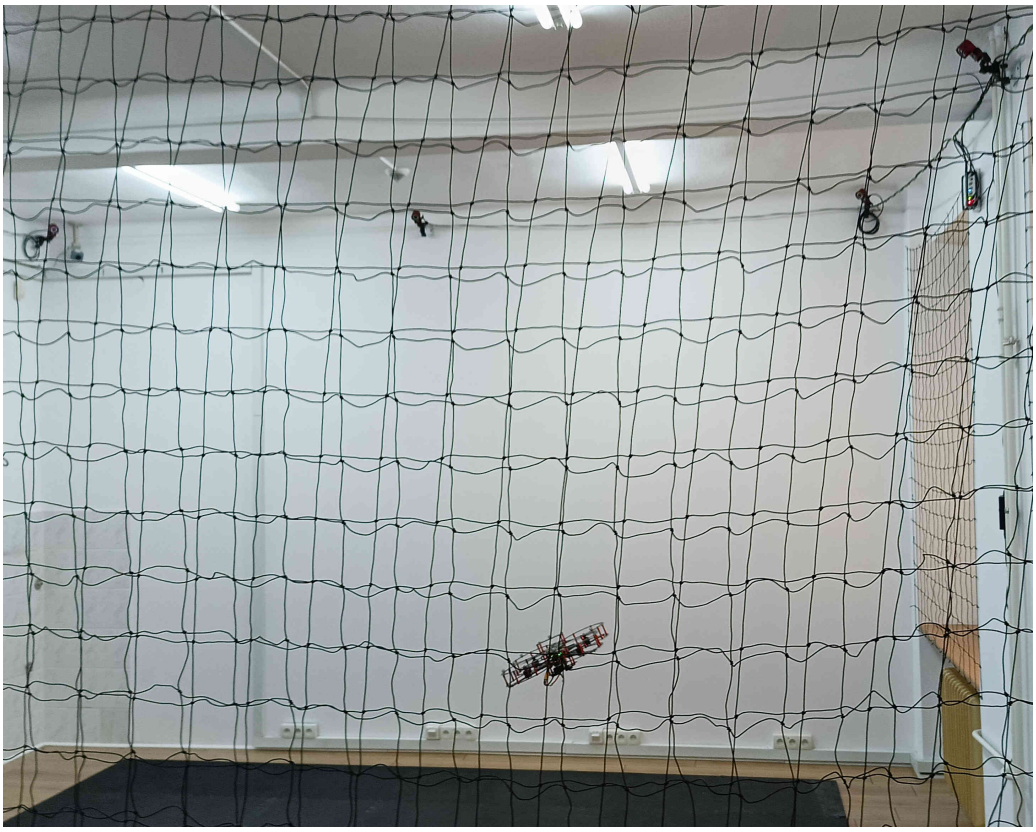

Figure 3 – Indoor flight test of the QDrone UAV in a controlled environment, surrounded by safety nets and tracked by the OptiTrack motion capture system.

The OptiTrack system provides highly accurate position and orientation measurements, which are critical for characterizing sensor errors and providing feedback for the control system. These measurements offer a substitute for GNSS-based data in outdoor environments, allowing for a more controlled study of the UAV's flight dynamics and the performance of the Kalman filter adaptation during aggressive maneuvers. Figure 3 depicts the setup for the indoor flight test, showcasing the QDrone operating within a controlled environment, surrounded by safety nets and monitored by the OptiTrack motion capture system.

4.3 Quadrotor Model

The dynamics of the QDrone quadrotor are modeled using well-established principles from the literature. For clarity, a concise summary is provided here to contextualize the system dynamics within the scope of this study. The quadrotor's motion is governed by a set of differential equations that describe both translational and rotational dynamics.

The dynamics of the quadrotor in the Earth-fixed reference frame are given by [8]:

$$\dot{\boldsymbol{r}} = \boldsymbol{R}_B^E \boldsymbol{v} \tag{12}$$

$$\dot{\boldsymbol{v}} = \frac{1}{m}\boldsymbol{F} - \boldsymbol{\omega} \times \boldsymbol{v} \tag{13}$$

$$\dot{\boldsymbol{\eta}} = \boldsymbol{J}\boldsymbol{\omega} \tag{14}$$

$$\dot{\boldsymbol{\omega}} = \boldsymbol{I}^{-1}(\boldsymbol{M} - \boldsymbol{\omega} \times \boldsymbol{I}\omega) \tag{15}$$

Here, $\boldsymbol{r}$ represents the position vector, $\boldsymbol{v}$ is the velocity, $\boldsymbol{\eta}$ refers to the Euler angles, and $\boldsymbol{\omega}$ is the angular velocity. These equations capture the linear and angular dynamics of the quadrotor. Specifically, Equation 12 describes the translational motion in the Earth-fixed frame, while equation 13 models the response of the quadrotor to forces in the body-fixed frame. Equation 14 governs the rotational motion, and Equation 15 details the angular response to moments acting on the vehicle.
The transformation matrix that converts coordinates from the body-fixed frame to the Earth-fixed frame is given by:
The transformation between the Earth-fixed and body-fixed frames is given by the rotation matrix $\boldsymbol{R}_B^E$, which converts coordinates from the body frame to the global frame:

$$\boldsymbol{R}_B^E = \begin{bmatrix} \cos\theta\cos\psi & -\cos\phi\sin\psi + \sin\psi\sin\theta\cos\psi & \sin\phi\sin\psi + \cos\phi\sin\theta\cos\psi \\ \cos\theta\sin\psi & \cos\phi\cos\psi + \sin\phi\sin\theta\sin\psi & -\sin\psi\cos\psi + \cos\phi\sin\theta\sin\psi \\ -\sin\theta & \sin\phi\cos\theta & \cos\phi\cos\theta \end{bmatrix} \tag{16}$$

This matrix is critical for translating the orientation of the quadrotor between reference frames, enabling accurate control and navigation. Additionally, the transformation from angular body rates to Euler angle rates is given by:

$$\boldsymbol{J} = \begin{bmatrix} 1 & \sin\phi\tan\theta & \cos\phi\tan\theta \\ 0 & \cos\phi & -\sin\phi \\ 0 & \sin\phi\sec\theta & \cos\phi\sec\theta \end{bmatrix} \tag{17}$$

The total force vector acting on the quadrotor consists of the inertial, propulsive, and aerodynamic forces:

$$\boldsymbol{F} = m\boldsymbol{R}_E^B \begin{bmatrix} 0 \\ 0 \\ g \end{bmatrix} + \begin{bmatrix} 0 \\ 0 \\ -T_c \end{bmatrix} - c_d\boldsymbol{v} \tag{18}$$

Here, T_c represents the total thrust generated by the four propellers:

$$T_c = T_1 + T_2 + T_3 + T_4 \tag{19}$$

The torques generated by the propellers contribute to the moments acting on the quadrotor:

$$M = \begin{bmatrix} L(T_3 - T_4) \\ L(T_2 - T_1) \\ -Q_1 - Q_2 + Q_3 + Q_4 \end{bmatrix} \tag{20}$$

Where L is the distance between the center of the quadrotor and each propeller, and Q_i represents the reaction torque generated by each propeller.
The quadrotor's response to external forces and moments is continuously monitored through onboard sensors. Accelerometers measure the specific forces acting on the vehicle, while gyroscopes track its angular rates in the body frame. These sensor readings are integrated into the state estimation process using established sensor models. The sensor input vector, representing accelerometer and gyroscope data, is given by:

$$\boldsymbol{u} = \begin{bmatrix} a_x,\ a_y,\ a_x,\ g_x,\ g_y,\ g_z \end{bmatrix} \tag{21}$$

The state vector $\boldsymbol{x}$, which includes the position, velocity, orientation, and sensor biases, is defined as:

$$\boldsymbol{x} = \left[x,\ y,\ z,\ u,\ v,\ w,\ \phi,\ \theta,\ \psi,\ b_{ax},\ b_{ay},\ b_{az},\ b_{gx},\ b_{gy},\ b_{gz}\right]^T \tag{22}$$

The state-space model for the quadrotor is then given by the following equations:

$$\dot{\boldsymbol{r}} = \boldsymbol{R}_B^E \boldsymbol{v} \tag{23}$$

$$\dot{\boldsymbol{v}} = \boldsymbol{a} - \boldsymbol{b}_a + \boldsymbol{R}_E^B \begin{bmatrix} 0 \\ 0 \\ g \end{bmatrix} - (\boldsymbol{g} - \boldsymbol{b}_g) \times \boldsymbol{v} \tag{24}$$

$$\dot{\boldsymbol{\eta}} = \boldsymbol{J}(\boldsymbol{g} - \boldsymbol{b}_g) \tag{25}$$

$$\dot{\boldsymbol{b}}_a = \boldsymbol{0} \tag{26}$$

$$\dot{\boldsymbol{b}}_g = \boldsymbol{0} \tag{27}$$

The Optitrack system provides accurate position and attitude feedback for the quadrotor, which is used in the measurement vector:

$$\boldsymbol{z} = \left[o_x,\ o_y,\ o_z,\ o_\phi,\ o_\theta,\ o_\psi\right]^T \tag{28}$$

This feedback ensures that the system remains observable and allows for precise estimation of the position, velocity, orientation, and sensor biases.

5. Results

5.1 Simulation Results

The QDrone, equipped with an OptiTrack motion capture system, was used to obtain high-precision measurements of the drone's position and orientation. These measurements served as ground truth data for evaluating the performance of two state estimation algorithms: the Extended Kalman Filter (EKF) and the Adaptive Kalman Filter (AKF). By comparing the filters' performance during dynamic UAV maneuvers, we aimed to assess how well each algorithm could track the UAV's state during periods of sudden changes in motion.

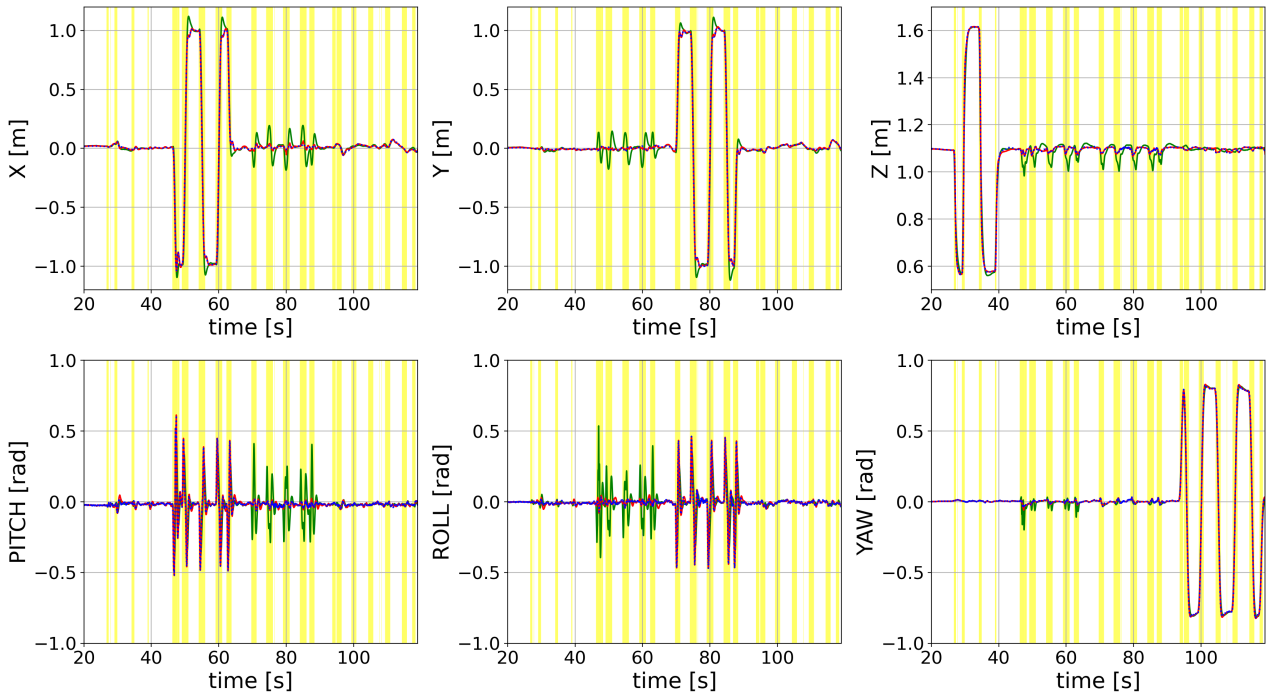

Figure 4 – Overall state estimation for X, Y, Z, pitch, roll, and yaw angles.

In Figure 4, the overall state estimation results are presented for both the EKF and AKF, showing the position states along the X, Y, Z axes, and the angular states—pitch, roll, and yaw. The comparison demonstrates how closely the filters' estimates align with the OptiTrack ground truth data, especially during periods of rapid motion. The highlighted yellow regions correspond to moments when the AKF detected a maneuver and dynamically adjusted its process noise covariance to adapt to the sudden motion. During these critical moments, the AKF shows better alignment with the ground truth data, particularly in yaw estimation, compared to the EKF.
Figures 5 through 10 provide a more detailed analysis of the filters' performance during specific maneuvers, focusing on time intervals where the UAV experienced significant motion along individual axes. These figures allow for a direct comparison of the state estimation quality between EKF and the AKF.
Figure 5 presents the estimation performance for a rapid acceleration along the X-axis. The AKF quickly adapts to the sudden increase in velocity, closely tracking the true motion of the UAV. In contrast, the EKF exhibits a lag in response, leading to less accurate position estimation during this phase. The period of detected motion is marked in yellow, indicating when the AKF's maneuver detection was triggered.

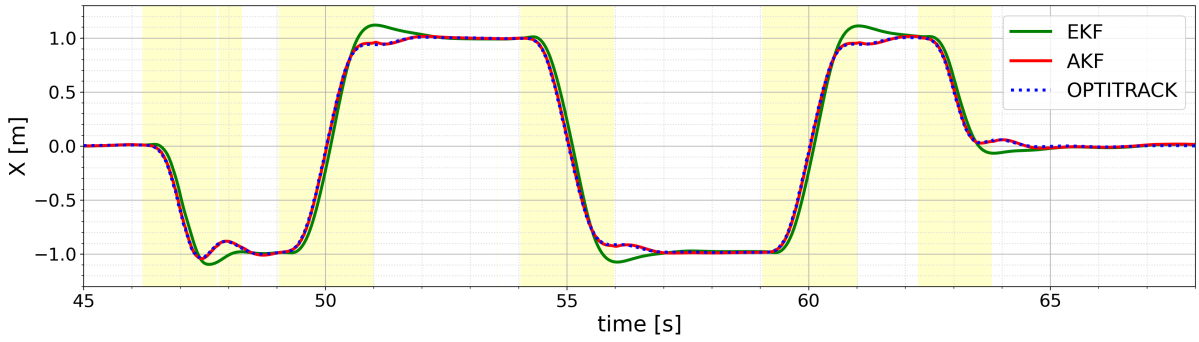

Figure 5 – State estimation during a sudden acceleration along the X-axis.

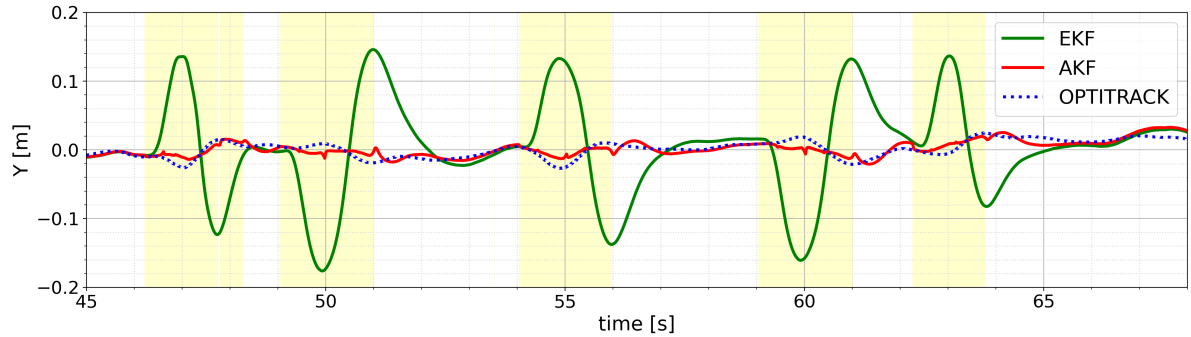

Figure 6 – State estimation along the Y-axis during motion in the X direction.

In Figures 6 and 7, we observe the state estimations along the Y and Z axes, respectively, during the same time interval as the X-axis motion in Figure 5. These figures reveal that while the UAV is accelerating in the X direction, fluctuations occur in the Y and Z axes for the EKF. These fluctuations represent estimation noise introduced during the rapid X-axis movement. The AKF, however, significantly reduces these fluctuations, demonstrating its ability to maintain accuracy across all axes during high-speed maneuvers in the X direction.
Figure 8 shows the UAV's behavior along the Y-axis during a similar event. Once again, the AKF's

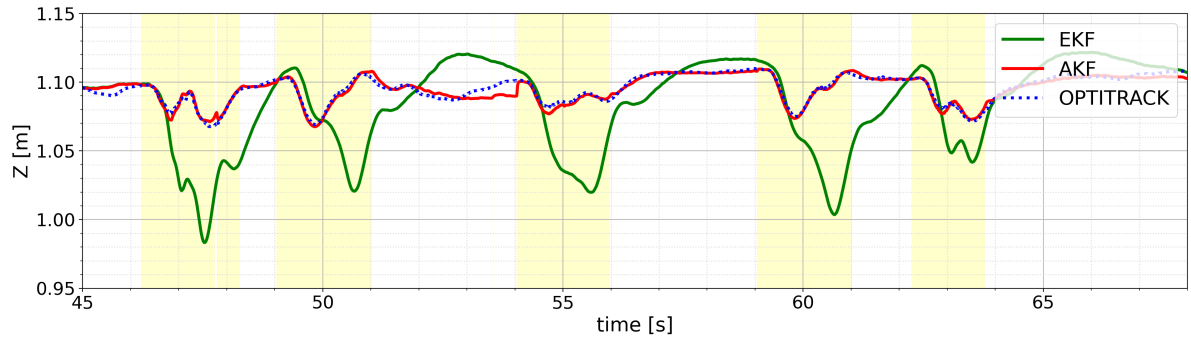

Figure 7 – State estimation along the Z-axis during motion in the X direction.

adaptive nature allows it to respond more effectively to the sudden acceleration, maintaining better alignment with the Optitrack data. The EKF lags behind during the maneuver, resulting in higher estimation errors.

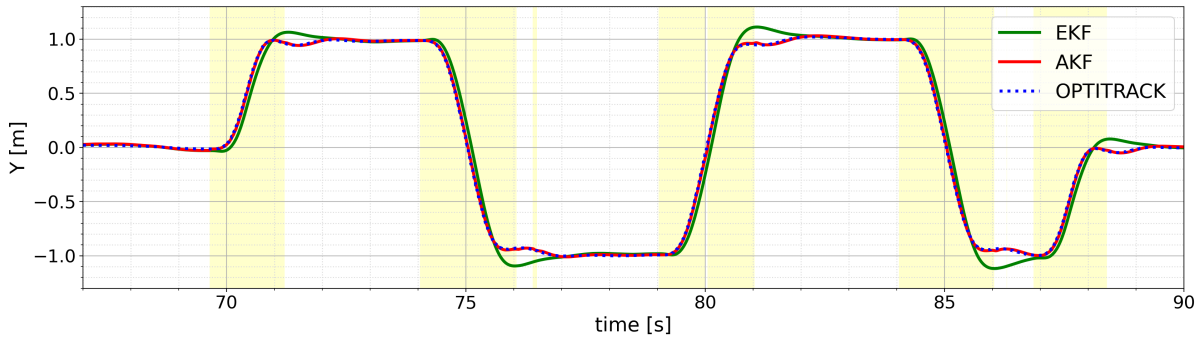

Figure 8 – State estimation during a sudden acceleration along the Y-axis

Figure 9 focuses on the UAV's Z-axis during a rapid change in vertical position. Here, the AKF's ability to dynamically adjust its process model ensures a more accurate estimation of the drone's altitude, even under aggressive movement. The EKF, on the other hand, exhibits greater deviations from the ground truth data during the highlighted maneuver phase, struggling to maintain accuracy.

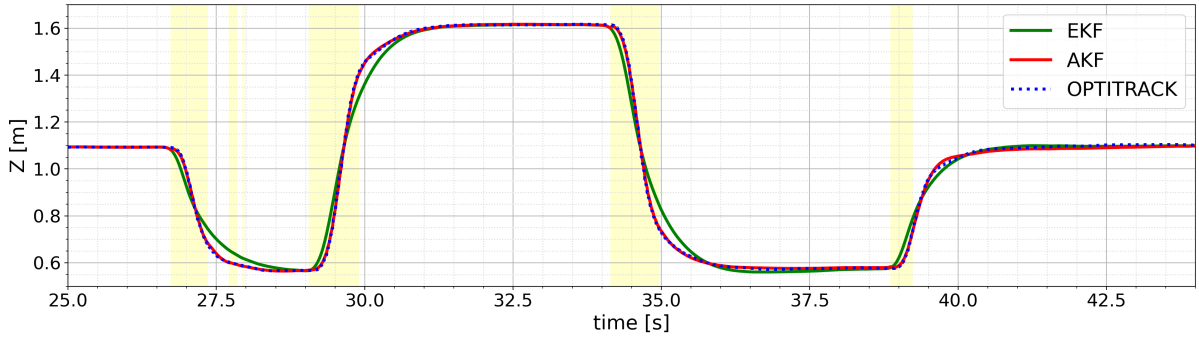

Figure 9 – State estimation during rapid vertical motion along the Z-axis

Figure 10 a sudden yaw rotation is examined. As the UAV undergoes a rapid change in its yaw

angle, the AKF quickly adapts to the sharp rotational movement, resulting in highly accurate yaw estimation. By contrast, the EKF fails to adjust as swiftly, showing a delayed response and larger errors. The yellow-shaded regions indicate the phases where the AKF detected and reacted to the sudden change in yaw.

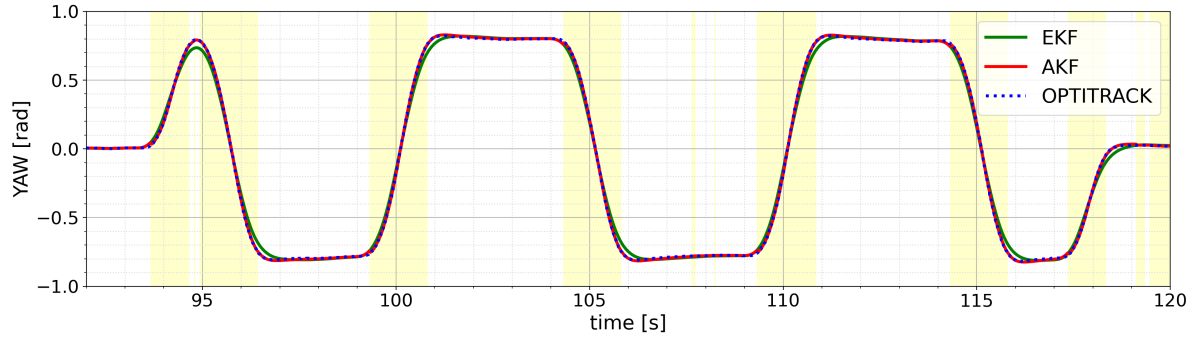

Figure 10 – State estimation during a sudden yaw movement

The Root Mean Square Error (RMSE) values, presented in the Table 1 below, further quantify the differences between the two filters. The AKF significantly outperforms the EKF in all state variables, particularly during phases of rapid movement, as seen in the lower RMSE values across the X, Y, Z, and yaw axes.

Table 1 – RMSE comparison between EKF and AKF across different state variables

Filter Type	RMSE X[m] Figure 5	RMSE Y[m] Figure 6	RMSE Z[m] Figure 7	RMSE Y[m] Figure 8	RMSE Z[m] Figure 9	RMSE YAW[rad] Figure 10
EKF	0.07817	0.07429	0.02930	0.08091	0.03104	0.02851
AKF	0.00867	0.00738	0.00282	0.00950	0.00558	0.00532

In all cases, the AKF demonstrates superior responsiveness and accuracy during rapid UAV movements compared to the EKF. This performance gain is primarily due to the AKF's dynamic adjustment of the process noise covariance, enabling it to more effectively track the UAV's state in real-time during aggressive maneuvers. The yellow-marked periods in the figures visually represent the moments where this adaptability provided a clear advantage over the EKF, particularly when the drone experienced sudden accelerations or rotations.

5.2 Discussion

The simulation results clearly demonstrate the advantages of the AKF over the Extended Kalman Filter. The root mean square error (RMSE) values were computed for each filter's estimated state, with the OptiTrack data serving as the reference. The RMSE comparison reveals that the AKF consistently achieved lower errors during periods of high dynamic activity as shown in Figure 4.

The primary advantage of the AKF is its capacity to dynamically adjust the process noise covariance in response to detected maneuvers. This adaptability allows the filter to respond effectively to sudden accelerations and rotations, maintaining a higher degree of accuracy. For instance, during rapid acceleration along the X-axis (Figure 5), the AKF quickly adapted to the changing velocity, providing a more precise estimation than the EKF. Additionally, as shown in Figures 6 and 7, while the UAV was moving along the X-axis, fluctuations appeared in the Y and Z estimations for the EKF, causing increased noise. These fluctuations were significantly reduced by the AKF, which maintained better stability across all axes during the X-axis motion. This highlights how the AKF's adaptability not only improves the accuracy of estimation in the primary direction of movement but also reduces noise in other state variables that are indirectly affected by rapid changes in motion.

Importantly, there is no trade-off in terms of computational time. The key challenge lies in determining the thresholds for maneuver detection, which may require some trial and error and adjustment based on the specific UAV dynamics. Once these thresholds are set, the AKF operates efficiently without introducing significant delays or requiring substantial additional processing power. This is a crucial distinction since it means the AKF can be implemented in real-time systems without the burden of excessive computation, provided that the maneuver detection parameters are carefully tuned.
In conclusion, the AKF offers significant improvements in estimation accuracy, especially during dynamic flight conditions occur. ts ability to adapt to maneuvers makes it a more robust solution for UAV state estimation compared to the standard Kalman Filter. The need for tuning the maneuver detection thresholds is the primary consideration for practical implementation, but it does not introduce prohibitive computational demands. This makes the AKF an effective and efficient choice for UAV systems requiring precise and reliable state estimation during aggressive maneuvers.

6. Conclusions

6.1 Summary of Findings

This study highlights the advantages of the Adaptive Kalman Filter (AKF) over the traditional Extended Kalman Filter (EKF) in estimating the state of a UAV during dynamic flight conditions. By dynamically adjusting the process noise covariance in response to detected maneuvers, the AKF offers significantly more accurate and responsive state estimation. The simulation results, validated against high-precision OptiTrack data, demonstrated that the AKF outperforms the EKF particularly in periods of rapid motion, such as sudden accelerations and sharp rotations. Across all axes—X, Y, Z, and yaw—the AKF consistently exhibited lower RMSE values, providing a clear advantage in maintaining the UAV's state accuracy during aggressive maneuvers. This adaptability makes the AKF a more robust solution for applications where quick and unpredictable movements are common, ensuring higher reliability in real-time UAV operations.

6.2 Future Work

Several avenues for future research remain. First, real-world testing of the AKF on physical UAV systems would further validate its performance beyond simulation environments. Such testing could reveal additional challenges and opportunities for fine-tuning the algorithm under various environmental conditions, such as wind or GPS signal loss. Moreover, further optimization of the maneuver detection algorithm, particularly in fine-tuning the thresholds for maneuver identification, could enhance the AKF's. Additionally, exploring the integration of more advanced sensor fusion techniques and machine learning models may further improve the filter's adaptability and overall performance in complex flight scenarios.

7. Contact Author Email Address

For any further inquiries or correspondence, please contact the author at:
kenan.majewski.dokt@edu.pw.pl

8. Copyright Statement

References

[1] Lyu M, Zhao Y, Huang C and Huang H. Unmanned Aerial Vehicles for Search and Rescue: A Survey. *Remote Sensing*, Vol. 15, No. 13, Article 3266, 2023. doi: 10.3390/rs15133266.

[2] Kalman R. A New Approach to Linear Filtering and Prediction Problems. *ASME Journal of Basic Engineering*, Vol. 82, pp. 35-45, 1960.

[3] Anderson B. D. O. and Moore J. B., *Optimal Filtering*. Prentice Hall, 1979.

[4] Marković L, Kovač M, Milijaš R, Car M and Bogdan S. Error State Extended Kalman Filter Multi-Sensor Fusion for Unmanned Aerial Vehicle Localization in GPS and Magnetometer Denied Indoor Environments. *Proc. of the 2022 International Conference on Unmanned Aircraft Systems (ICUAS)*, Dubrovnik, Croatia, pp. 184-190, 2022. doi: 10.1109/ICUAS54217.2022.9836124.

[5] Luo Y, Ye G, Wu Y, Guo J, Liang J and Yang Y. An Adaptive Kalman Filter for UAV Attitude Estimation. *2019 IEEE 2nd International Conference on Electronics Technology (ICET)*, Chengdu, China, pp. 258-262, 2019. doi: 10.1109/ELTECH.2019.8839496.

[6] Chang G. Robust Kalman filtering based on Mahalanobis distance as outlier judging criterion. *Journal of Geodesy*, Vol. 88, pp. 391–401, 2014. doi: 10.1007/s00190-013-0690-8.

[7] Elya M, Noor S, Zafira A, and Azrad S. Implementation of Extended High-Gain Observer in Low-Cost OptiTrack Motion Tracking System for UAV Control. *2017 IEEE 15th Student Conference on Research and Development (SCOReD)*, pp. 29-34, 2017. doi: 10.1109/SCORED.2017.8305426

[8] Ireland M and Anderson D. Development of Navigation Algorithms for Nap-of-the-Earth UAV Flight in a Constrained Urban Environment. *Proc. of the 5th Conference on Navigation Algorithms*, Vol. 5, 2012.